ARTICLE

Supporting Information – Improved Thermoelectric Efficiency of $Sb_2Si_2Te_6$ Through Yttrium Induced Nanocompositing

Received 00th January 20xx,
Accepted 00th January 20xx

DOI: 10.1039/x0xx00000x

Kivanc Saglik[a,b,#], Xian Yi Tan[a,b,#], Jinfeng Dong[a,#], Ady Suwardi[c], Xizu Wang[b], Jianwei Xu[d], Qiang Zhu[b,d], Hongfei Liu[b], Jing Cao[b,*] and Qingyu Yan[a,*]

Structural Characterization

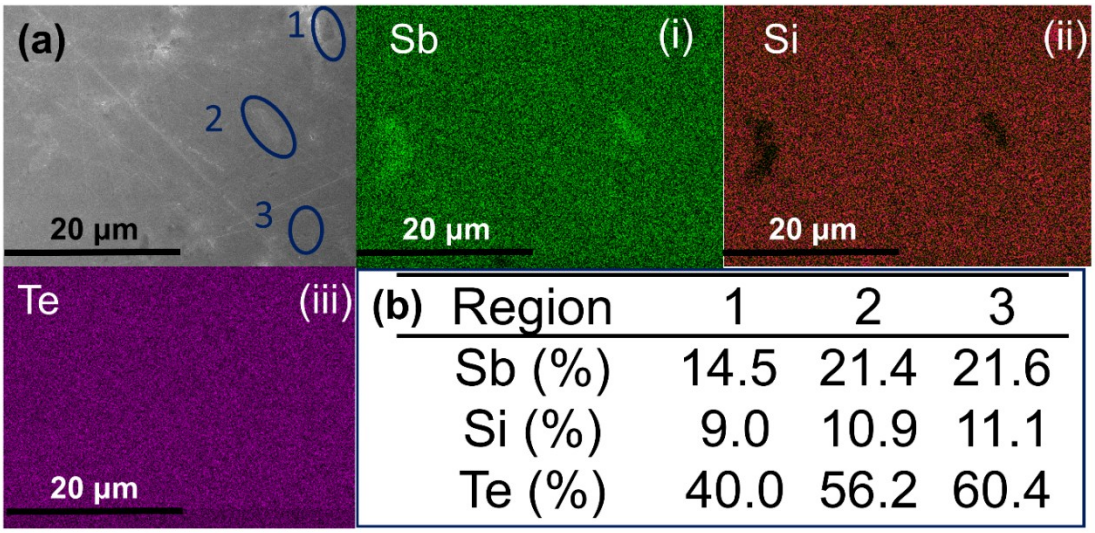

(b)

Region	1	2	3
Sb (%)	14.5	21.4	21.6
Si (%)	9.0	10.9	11.1
Te (%)	40.0	56.2	60.4

Fig. S1 (a) The FESEM image of $Sb_2Si_2Te_6$. Elemental mapping images showing the distribution of (i) Sb, (ii) Si, and (iii) Te (b) Detailed quantification results revealing the atomic percent of each element.

[a.] *School of Materials Science and Engineering, Nanyang Technological University, 50 Nanyang Ave, Block N4.1, 639798, Singapore.*
E-mail: alexyan@ntu.edu.sg
[b.] *Institute of Materials Research and Engineering (IMRE). Agency for Science, Technology, and Research (A*STAR), 2 Fusionopolis Way, 138634, Singapore.*
E-mail: cao_jing@imre.a-star.edu.sg
[c.] *Department of Electrical Engineering, The Chinese University of Hong Kong (CUHK), Central Ave, Hong Kong, 999077*
[d.] *Institute of Sustainability for Chemicals, Energy, and Environment (ISCE2), Agency for Science, Technology, and Research, (A*STAR), 1 Pesek Road, Jurong Island, 627833, Singapore*
[#] Contributed equally.
* Corresponding authors.
† Supplementary Information available: [details of any supplementary information available should be included here]. See DOI: 10.1039/x0xx00000x

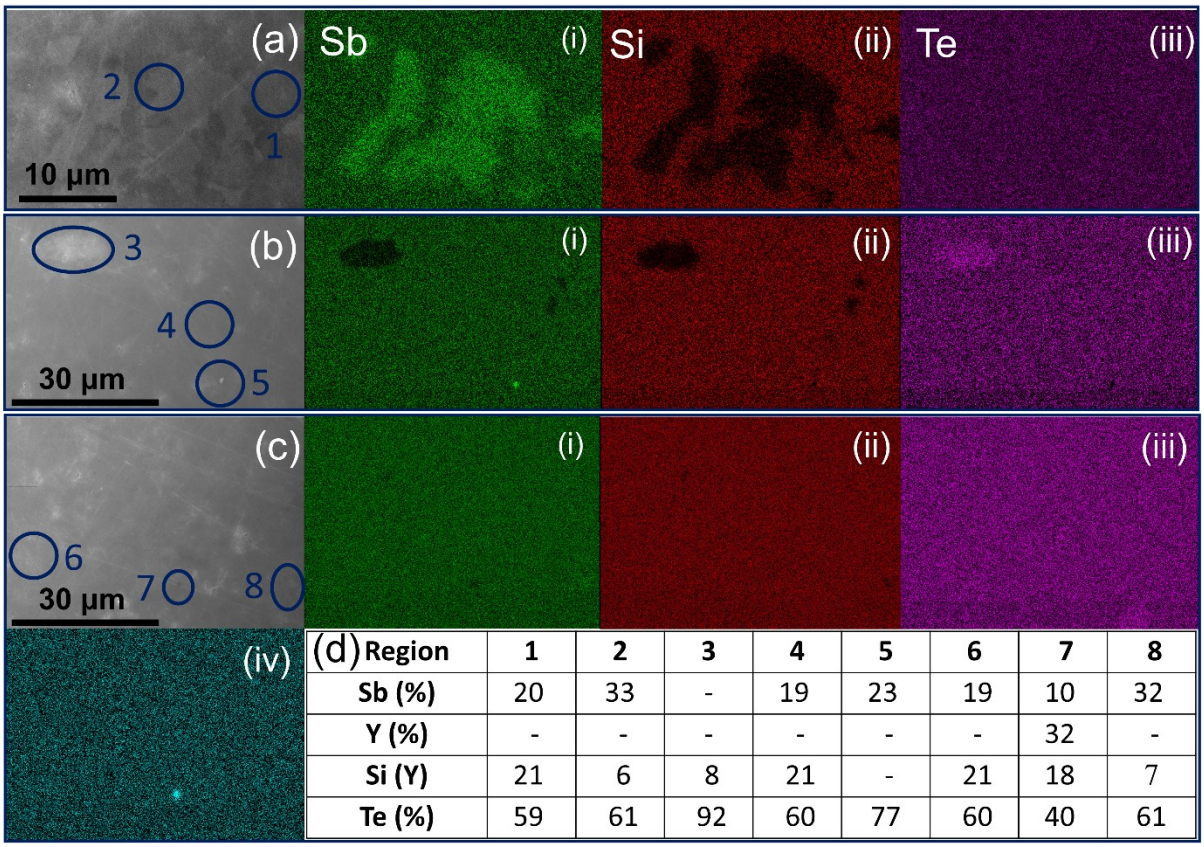

(d)

Region	1	2	3	4	5	6	7	8
Sb (%)	20	33	-	19	23	19	10	32
Y (%)	-	-	-	-	-	-	32	-
Si (Y)	21	6	8	21	-	21	18	7
Te (%)	59	61	92	60	77	60	40	61

Fig. S2 (a), (b), (c), the FESEM images of $Sb_{1.98}Y_{0.02}Si_2Te_6$. Elemental mapping images showing es showing the distribution of (i) Sb, (ii) Si, (iii) Te and (iv) Y. (d) Detailed quantification results revealing the atomic percent of each element.

The nominal compositions of $Sb_{2-x}Y_xSi_2Te_6$ were analyzed using EDS and XRF techniques. The findings are summarized in Table S1.

Table S2 Nominal, EDS determined and XRF determined compositions of $Sb_{2-x}Y_xSi_2Te_6$.

Nominal Composition	Composition from EDS	Composition from XRF
$Sb_2Si_2Te_6$	$Sb_{1.64}Si_2Te_{5.09}$	$Sb_{1.79}Si_2Te_{5.85}$
$Sb_{1.99}Y_{0.01}Si_2Te_6$	-	$Sb_{1.81}Y_{0.016}Si_2Te_{5.71}$
$Sb_{1.98}Y_{0.02}Si_2Te_6$	$Sb_{1.71}Y_{0.042}Si_2Te_{5.36}$	$Sb_{1.71}Y_{0.022}Si_2Te_{5.42}$
$Sb_{1.97}Y_{0.03}Si_2Te_6$	-	$Sb_{1.77}Y_{0.030}Si_2Te_{5.61}$

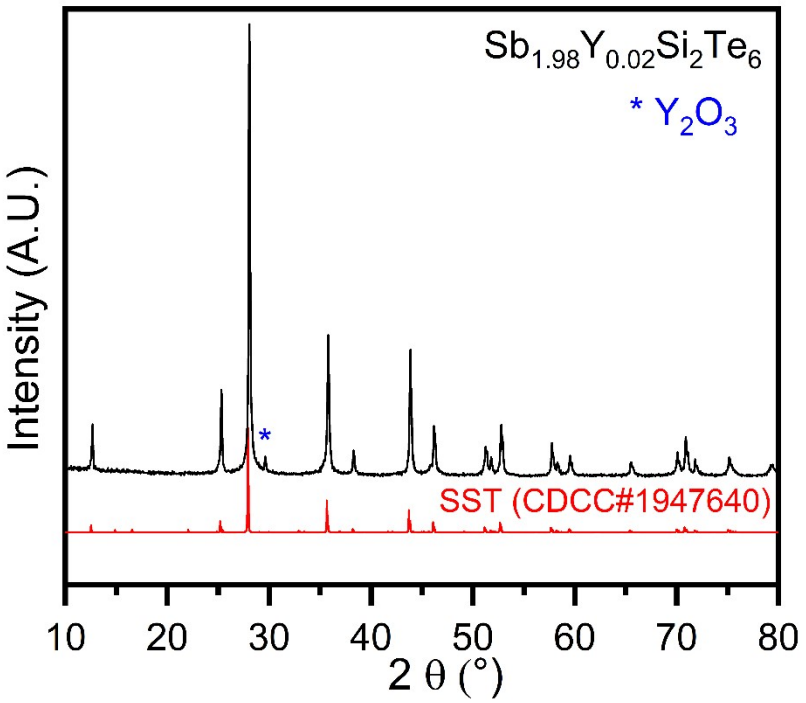

Fig. S3 Powder X-ray diffractogram of $Sb_{1.98}Y_{0.02}Si_2Te_6$, spanning from 2θ=10 – 80.

Rietveld Refinement

In the Rietveld refinement, the structural model used was based on the Rietveld method. A Pseudo – Voigt function was applied to model the peak shapes and a linear interpolation approach was used for the background fitting. The Rietveld Refinement Quality indicators (Chi^2, R_p, R_{wp}, R_{exp}) of $Sb_{2-x}Y_xSi_2Te_6$ are reported in Table S2.

Table S3 The Rietveld Refinement quality factors of $Sb_{2-x}Y_xSi_2Te_6$ samples.

Nominal Composition	Chi^2	R_p	R_{wp}	R_{exp}
$Sb_2Si_2Te_6$	8.94	25.3	25.5	8.53
$Sb_{1.99}Y_{0.01}Si_2Te_6$	5.89	22.1	21.4	8.81
$Sb_{1.98}Y_{0.02}Si_2Te_6$	5.92	16.2	16.8	8.81
$Sb_{1.97}Y_{0.03}Si_2Te_6$	5.43	18.8	19.1	8.20

The graphical representations of the Rietveld Refinements of $Sb_{2-x}Y_xSi_2Te_6$ are reported in Fig S4.

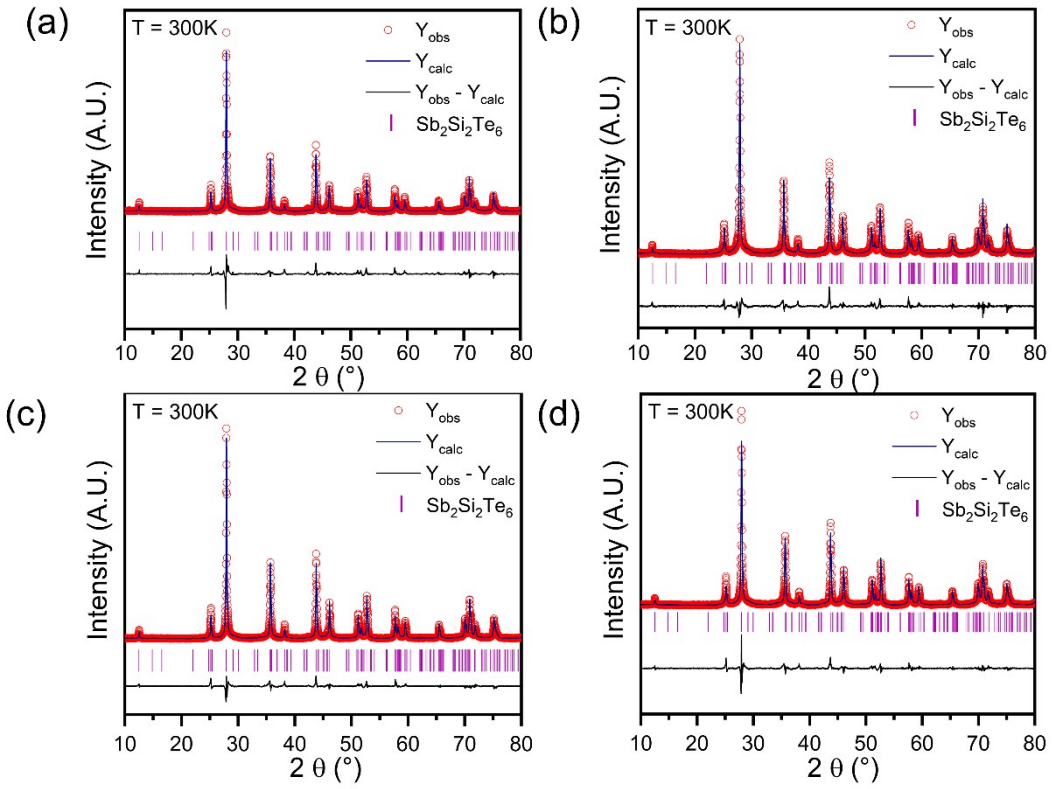

Fig. S4 The graphical representation of Rietveld Refinement of (a) $Sb_2Si_2Te_6$, (b) $Sb_{1.99}Y_{0.01}Si_2Te_6$, (c) $Sb_{1.98}Y_{0.02}Si_2Te_6$, (d) $Sb_{1.97}Y_{0.03}Si_2Te_6$.

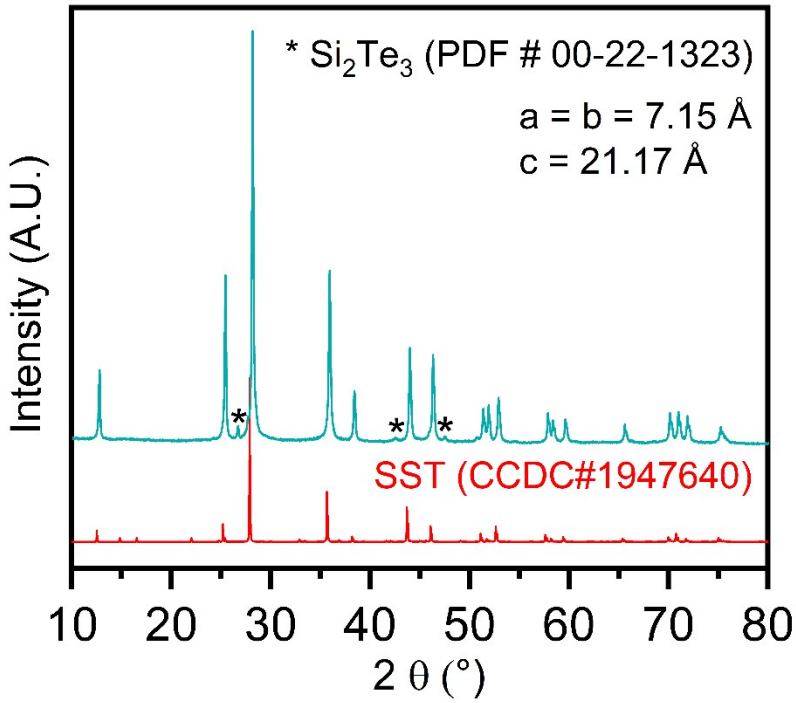

Fig. S5 Powder X-ray diffractogram of $Sb_{1.96}Y_{0.04}Si_2Te_6$ spanning from 2θ=10 – 80

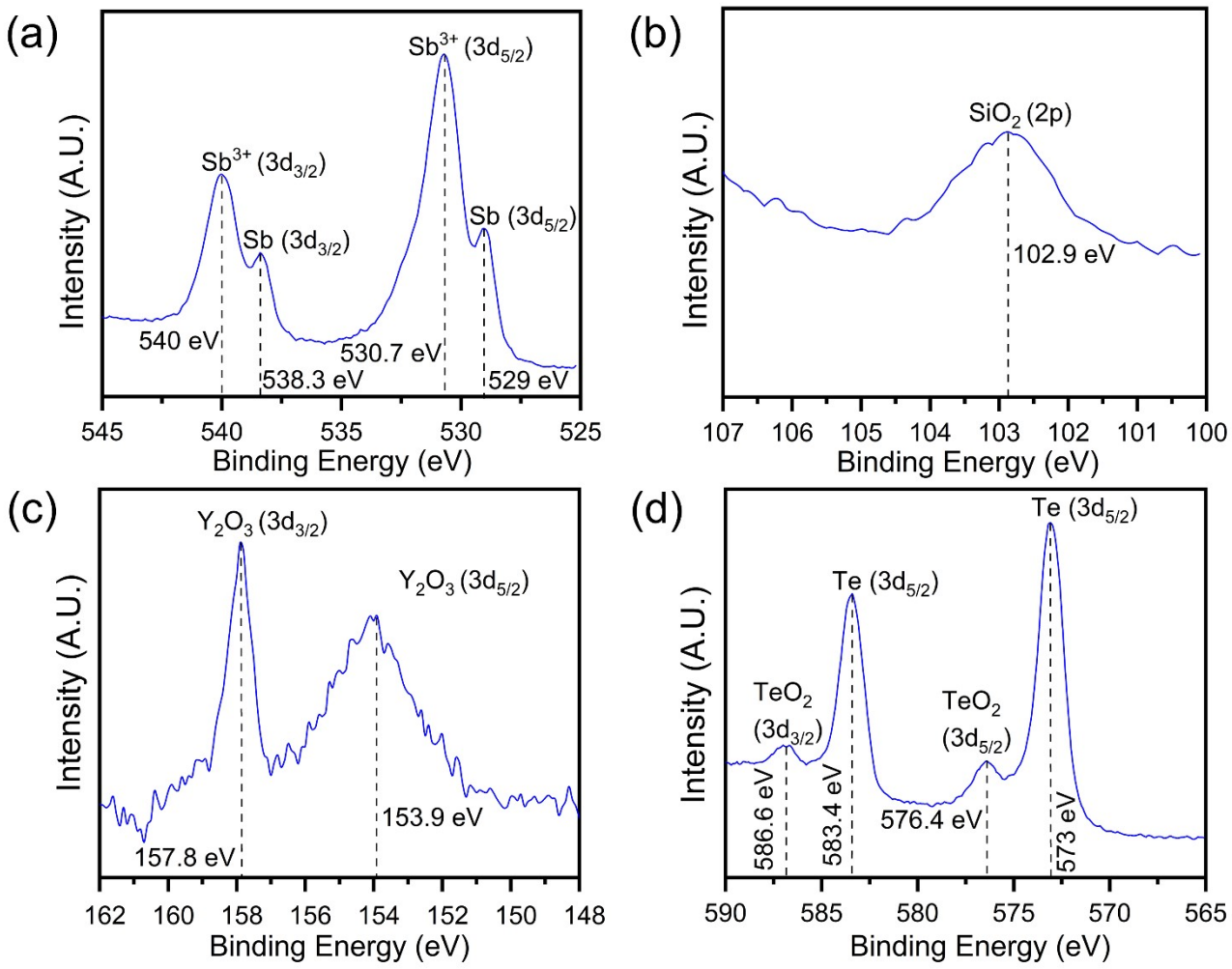

Fig. S6 XPS survey spectra for $Sb_{1.98}Y_{0.02}Si_2Te_6$, reporting binding energies of (a) Sb, (b) Si, (c) Y, and (d) Te

Lattice Thermal Conductivity Modeling

Lattice thermal conductivity of materials is heavily affected by the Umklapp processes, grain boundaries and point defects. Debye Callaway modeling is useful for revealing the contributions of each phonon scattering mechanism, and has been heavily utilized so far[1]. In this model, the lattice thermal conductivity is calculated through integrating the spectral lattice thermal conductivity (κ_s) over the whole frequency range, as in Equation 1. Table S3 shows the values of parameters whose calculations are not explained in this chapter.

$$\kappa_s(\omega) = \frac{1}{3}\int_0^{\omega_D} C_s(\omega) v^2 \tau(\omega) d\omega \quad (1)$$

Here, ω, $C_s(\omega)$, υ, and τ refer to the phonon frequency, spectral heat capacity, average speed of sound, and total phonon relaxation time respectively.
The phonon frequency, ω, is calculated as follows:

$$\omega = \left(\frac{6\pi^2}{\Omega}\right).\upsilon \tag{2}$$

Here, Ω refer to average atomic volume. The average speed of sound (υ) has the contributions from transverse (υ_T) and longitudinal (υ_L) speed of sound, calculated as follows:

$$\upsilon = \left[\frac{1}{3}\left(\frac{1}{\upsilon_L{}^3}\right) + \left(\frac{2}{\upsilon_T{}^3}\right)\right]^{-1/3} \tag{3}$$

The spectral heat capacity (C_s) could be expressed as follows:

$$C_s(\omega) = \frac{3k_B\omega^2}{2\pi^2\upsilon^3} \tag{4}$$

To calculate the total phonon scattering rate (τ^{-1}), the individual phonon scattering rates of all scattering mechanisms should be summed up as follows:

$$\tau^{-1} = \tau_U^{-1} + \tau_{GB}^{-1} + \tau_{PD}^{-1} \tag{5}$$

Here, τ_U^{-1}, τ_{GB}^{-1}, and τ_{PD}^{-1} refer to the Umklapp, Grain boundary, and Point defect scattering rates, respectively.
The Umklapp phonon scattering rate is calculated as follows:

$$\tau_U^{-1} = A_N.\frac{2}{(6\pi^2)^{1/3}}.\frac{k_B\Omega^{1/3}\gamma^2\omega^2T}{\bar{M}\upsilon^3} \tag{6}$$

Here, γ, and $\bar{M}$, and A_N refer to Grüneisen parameter, average atomic mass, and the integration coefficient between Umklapp and Normal processes, respectively.

The grain boundary scattering rate is expressed as follows:

$$\tau_{GB}^{-1} = \frac{\upsilon}{d} \tag{7}$$

Where d is the average grain size.

Finally, the point defect scattering rate is calculated through equation 8:

$$\tau_{PD}^{-1} = \frac{\Omega\omega^4}{4\pi\upsilon^3}.\Gamma \tag{8}$$

Here, Γ refers to the point defect scattering parameter, and it is manually optimized to find the best fit between modeled and real lattice thermal conductivity.

The thermal conductivity in terms of temperature could be expressed as follows:

$$\kappa_L(T) = \frac{k_B}{2\pi^2\upsilon}\left(\frac{k_BT}{\hbar}\right)^3\int_0^{\theta_D/T}\tau(x)\frac{x^4exp(x)}{[\exp(x)-1]^2}dx \tag{9}$$

Here, k_B, ħ, and θ_D refer to Boltzmann constant, Planck's constant, and Debye temperature, respectively. "x" could be expressed as follows:

$$x = \frac{\hbar\omega}{k_B T} \tag{10}$$

The Debye temperature, θ_D, is calculated as follows:

$$\theta_D = \frac{\hbar\omega}{k_B} \tag{11}$$

Debye – Cahill Model

Assuming a material has totally an amorphous structure, the lattice thermal conductivity attains a minimum value called as amorphous limit ($\kappa_{L,min}$). This minimum value has been heavily calculated[1-3] by using the following equation.

$$\kappa_{L,min} = \left(\frac{\pi}{6}\right)^{1/3} k_B n_a^{2/3} \sum_i v_i \left(\frac{T}{\theta_i}\right)^2 \int_0^{\theta_i/T} \frac{x^3 e^x}{(e^x - 1)^2} dx \tag{12}$$

Where θ_i is expressed as:

$$\theta_i = v_i \left(\frac{\hbar}{k_B}\right) 6\pi^2 n_a \tag{13}$$

Table S3 Parameters used for Debye Callaway and Debye Cahill models.

Symbol	Parameter	Value	Reference
Ω	Average volume per atom	3.26×10^{-29} m^3	3
υ_L	Longitudinal sound velocity	2450 m/s	4
υ_T	Transverse sound velocity	1250 m/s	4
A_N	Integration coefficient between Umklapp and Normal scattering processes	2	2
ϒ	Gruneisen parameter	2.98	2
Γ	Point defect scattering parameter	0.36	fitted
n_a	Number density of atoms	1.06×10^{28} m^{-3}	2

Modeling of Thermoelectric Figure of Merit

The highest zT achievable upon the optimization of carrier concentration can be evaluated through the quality factor (B) and reduced Fermi level (η). This section will elaborate B and η[5].

Quality Factor (B)

Quality factor is a carrier concentration independent property, and can be calculated as follows:

$$B = \left(\frac{k_B}{e}\right)^2 \frac{\sigma_{E0}}{\kappa_L} T \tag{14}$$

Here, σ_{E0} is the electronic transport coefficient which is calculated as follows

$$\sigma_{E0} = \sigma.exp\left(\frac{|S|}{\kappa_B/e} - 2\right) \quad (15)$$

The knowledge of σ_{E0} helps explain how the intrinsic electrical transport of the material is affected.

Reduced Fermi level (η) and Single Parabolic Band (SPB) Model

SPB model assumes that acoustic phonon scattering is the dominant scattering mechanism. According to the SPB model, the Fermi integrals ($F_i(\eta)$) could be calculated as follows[6]:

$$F_i = \int_0^\infty \frac{\in^i d \in}{1 + exp(\in - \eta)} \quad (16)$$

Here, $\in$ and η refer to reduced energy of the carrier and the reduced Fermi energy, respectively. The reduced Fermi energy is expressed as follows:

$$\eta = \frac{E_F}{k_B T} \quad (17)$$

Despite carrier concentration measurements prone to inaccuracies due to magnetic field, the reduced Fermi energy could be calculated by using the Seebeck coefficient of the material, through using the following formula:

$$S(\eta) = \mp \frac{k_B}{e}\left[\eta - \frac{\left(r + 5/2\right)F_{r+1.5(\eta)}}{\left(r + 3/2\right)F_{r+0.5(\eta)}}\right] \quad (18)$$

After finding the reduced Fermi energy values corresponding to Seebeck coefficient values, the Lorenz number of each sample at various temperature points could be calculated using the following formula.

$$L(\eta) = \left(\frac{k_B}{e}\right)^2\left[\frac{\left(r + 7/2\right)F_{r+1.5(\eta)}}{\left(r + 5/2\right)F_{r+0.5(\eta)}} - \left(\frac{\left(r + 5/2\right)F_{r+1.5(\eta)}}{\left(r + 3/2\right)F_{r+0.5(\eta)}}\right)^2\right] \quad (19)$$

The Lorenz number values obtained here were used to calculate the electronic thermal conductivity of the samples in this study.

$$\kappa_e = L.\sigma.T \quad (20)$$

Finally, the thermoelectric figure of merit (*zT*) in terms of reduced Fermi energy is calculated through the following formula:

$$zT(\eta) = \frac{S^2\eta}{\frac{(k_B/e)^2}{B_{TE}.F_{r+0.5}(\eta)} + L(\eta)} \quad (21)$$

The quality factor values obtained by equation (16) could be added to the plot of *zT* vs *η* to comment on possible mechanisms to enhance the *zT* values.

References

1. X. Y. Tan, J. Dong, J. Liu, D. Zhang, S. F. D. Solco, K. Sağlık, N. Jia, I. J. W. J. You, S. W. Chien and X. Wang, *Advanced Science*, 2024, 2400870.
2. H. Jang, S. Abbey, B. Frimpong, C. V. Nguyen, P. Ziolkowski, G. Oppitz, M. Kim, J. Y. Song, H. S. Shin and Y. S. Jung, *ACS Applied Materials & Interfaces*, 2022, **14**, 1270-1279.
3. C. Chen, D. Shen, C. Xia, Z. Zhang, W. Wang, Q. Zhang and Y. Chen, *Chemical Engineering Journal*, 2022, **441**, 135968.
4. Y. Luo, S. Cai, S. Hao, F. Pielnhofer, I. Hadar, Z.-Z. Luo, J. Xu, C. Wolverton, V. P. Dravid, A. Pfitzner, Q. Yan and M. G. Kanatzidis, *Joule*, 2020, **4**, 159-175.
5. S. D. Kang and G. J. Snyder, *arXiv preprint arXiv:1710.06896*, 2017.
6. J. de Boor, A. Berche and P. Jund, *The Journal of Physical Chemistry C*, 2020, **124**, 14987-14996.